Journal of Mines, Metals and Fuels, *73(11): 3589-3598; 2025. DOI: 10.18311/jmmf/2025/50001*

Print ISSN : 0022-2755

Journal of Mines, Metals and Fuels

Contents available at: *www.informaticsjournals.co.in/index.php/jmmf*

A Non-Destructive Approach to Characterize Nodularity in SG Iron Castings using Ultrasonic Testing

Digvijay Mhamane[1*] and Anand Bewoor[2]

[1]Department of Mechanical Engineering, Zeal College of Engineering and Research, Narhe Pune, Savitribai Phule Pune University, Pune - 411041, Maharashtra, India; digvijay.ndt@gmail.com

[2]Cummins College of Engineering for Women, Pune - 411052, Maharashtra, India

Abstract

This study presents a comprehensive, non-destructive approach for evaluating nodularity in SG iron castings by integrating ultrasonic testing and microstructural analysis. The investigation focuses on three SG iron grades (400/12, 500/7, and 600/3) produced under varying casting conditions, including pouring temperatures (1380° C, 1400° C, 1420° C), carbon equivalent values (4.6, 4.3, 4.0), and section thicknesses (5 mm, 10 mm, 15 mm). Ultrasonic velocity measurements were carried out using the ultrasonic flaw detector with a 4 MHz transducer. Complementing this, microstructural examination of samples was conducted using an inverted trinocular microscope to validate nodularity levels. A linear regression model incorporating process parameters achieved a high predictive accuracy (R^2 = 0.8955). Microstructural analysis using an inverted trinocular microscope confirmed the reliability of ultrasonic results, showing consistent trends in nodularity evaluation. The study confirms that ultrasonic testing is a reliable, efficient, and cost-effective tool for assessing nodularity in SG iron castings.

Major Findings: *Nodularity showed strong correlation with ultrasonic velocity, and a regression model (R^2 = 0.8955) accurately predicted it using velocity, PT, CEV, and thickness. Higher PT (1420° C) and lower CEV (4.0) enhanced nodularity. Ultrasonic results closely matched microscopy, ensuring fast, cost-effective evaluation.*

Keywords: *Material Characterization, Nodularity Evaluation, Non-destructive Testing (NDT), SG Iron Castings, Ultrasonic Testing*

1.0 Introduction

Spheroidal Graphite (SG) iron, also known as ductile iron, is a versatile material widely used in engineering applications due to its superior mechanical properties such as high strength, toughness, and ductility. These properties are primarily influenced by the nodularity of graphite within the iron matrix, which determines the material's ability to withstand mechanical stresses. Ensuring an optimal degree of nodularity is therefore critical for achieving consistent performance in SG iron castings[1-3]. Traditionally, nodularity assessment is performed through metallographic analysis, which involves destructive testing methods. While effective, these methods are time-intensive, costly, and impractical for large-scale or on-site evaluations. In contrast, ultrasonic testing provides a non-destructive, efficient, and reliable alternative by utilizing the correlation between ultrasonic velocity and material microstructure. Despite its advantages, the application of ultrasonic techniques for nodularity assessment in SG iron remains underexplored[4].

**Author for correspondence*

Furthermore, while the Design of Experiments (DOE) methodology has proven to be an effective tool for optimizing multi-variable systems[5], limited studies have combined ultrasonic testing with a DOE framework to investigate the factors influencing nodularity and ultrasonic velocity. This gap in research presents an opportunity to develop a systematic approach for characterizing SG iron castings. The objective of this study is to bridge this gap by correlating ultrasonic velocity with percentage nodularity in SG iron castings using an L27 orthogonal array within the DOE framework[6,7]. This approach not only facilitates the identification of significant factors affecting nodularity but also enhances the efficiency and accuracy of quality control processes in SG iron production[8].

2.0 Materials and Methods

2.1 Material Configurations

The study was conducted on SG iron grades SGI 400/12, SGI 500/7, and SGI 600/3, which represent a range of mechanical properties suitable for various industrial applications. The important elements that contribute to the manufacturing of spheroidal graphite, such as Carbon (C), Silicon (Si), and Phosphorous (P), are highlighted in Table 1, which summarises the compositions of these grades utilised for actual casting and falls within the specified range of these grades[9].

The castings were prepared using step casting molds designed to produce specimens with varying thicknesses (5 mm, 10 mm, 15 mm) to simulate different cooling rates and solidification conditions. This approach ensured a diverse range of microstructures and nodularity levels across the samples. The base iron was melted in an induction furnace and tapped at a temperature of approximately 1380-1420° C. Sand molds with step casting cavities were used, allowing controlled cooling rates across sections of varying thickness. The molten metal was poured at a temperature of 1380-1420° C to ensure proper filling and avoid casting defects. The castings were allowed to cool in the mold to ambient temperature.

3.0 Experimental Design

This study adopts a structured Design of Experiments (DOE) approach to investigate the influence of multiple factors on the ultrasonic velocity and percentage nodularity in SG iron castings. The experimental framework is based on the L27 orthogonal array, which enables the study of three control factors at three levels while minimizing the number of experiments required.

The Carbon Equivalent Value (CEV) is a measure used to assess the overall influence of carbon and other alloying elements on the properties of cast iron. For SG iron (ductile iron), the CEV is calculated using the following Equation (1) and summarized in Table 2[10].

$$CEV = \%C + \frac{1}{3}\ (\%Si + \%P) \qquad (1)$$

Where: % C = Percentage of Carbon, % Si = Percentage of Silicon, % P = Percentage of Phosphorus.

The input parameters and their levels are shown in Table 3. For conducting the experiments pouring temperature is varied from 1380° C to 1420° C for the step casting whose section thickness varies from 5 mm to 15 mm. The L27 orthogonal array by using three parameters and three levels is prepared by the Taguchi method in Minitab software and is expressed in Table 4[6]. For every experimental trial, the same geometry of casting consisting of variable section thickness will be simulated.

3.1 Actual Casting Trials

Following the L27 orthogonal array, a series of casting trials have been conducted to explore the effects of varying parameters on the casting process. The orthogonal array

Table 1. Chemical composition of SG iron grades

SG Iron Grades		C %	Si %	Mn %	P %	S %	Mg %	Cu %
400/12	Actual	3.65	2.825	0.66	0.045	0.021	0.035	-
500/7	Actual	3.45	2.62	0.45	0.045	0.018	0.035	0.4
600/3	Actual	3.25	2.36	0.66	0.045	0.020	0.035	0.4

Where; SG - Spheroidal Graphite, 400 - Tensile Strength (N/mm^2), 12 - % elongation.

Table 2. Carbon Equivalent Value (CEV) representing SG iron grades

SGI Grade	%C	%Si	%P	Carbon Equivalent Value (CEV)
400/12	3.65	2.825	0.045	4.60
500/7	3.45	2.62	0.045	4.30
600/3	3.25	2.36	0.045	4.00

Table 3. The input parameters and their levels

S. No	Parameter	Short-form	Level-I	Level-II	Level-III
1	Pouring temperature (°C)	PT	1380	1400	1420
2	Carbon Equivalent Value (CEV)	CEV	4.6	4.3	4.0
3	Section thickness (mm)	T	5	10	15

Table 4. L27 orthogonal array

Expt. No.	PT (°C)	CEV	T (mm)
1	1380	4.6	5
2	1380	4.6	10
3	1380	4.6	15
4	1380	4.3	10
5	1380	4.3	15
6	1380	4.3	5
7	1380	4.0	15
8	1380	4.0	5
9	1380	4.0	10
10	1400	4.6	5
11	1400	4.6	10
12	1400	4.6	15
13	1400	4.3	10
14	1400	4.3	15
15	1400	4.3	5
16	1400	4.0	15
17	1400	4.0	5
18	1400	4.0	10
19	1420	4.6	5
20	1420	4.6	10
21	1420	4.6	15
22	1420	4.3	10
23	1420	4.3	15
24	1420	4.3	5
25	1420	4.0	15
26	1420	4.0	5
27	1420	4.0	10

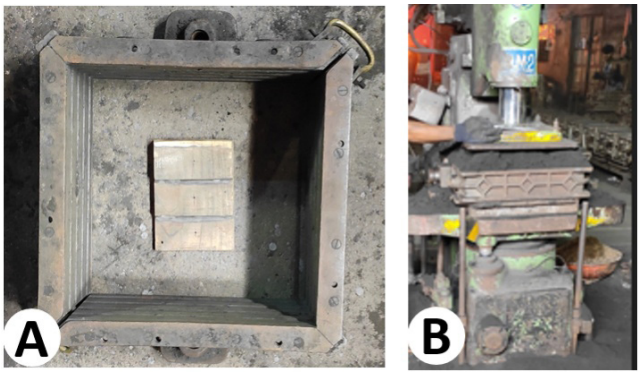


Figure 1. Molding operation **(A)** Preparation of drag **(B)** Machine molding.

provides a structured approach to testing different combinations of pouring temperatures, grades of SG iron, and sectional thicknesses. Each experiment was carefully executed to ensure precise control over the parameters. Samples from these trials are prepared for analysis, aiming to assess how these different conditions influence the quality and properties of the castings. This structured approach enables a detailed evaluation of how each parameter affects the casting process, ultimately providing valuable insights into optimizing the casting conditions for improved performance. Figure 1 to 4 represents the various steps involved in the actual casting trials and casting samples.

4.0 Ultrasonic Testing

The Ultrasonic Velocity (UV) measurements were conducted using the ADVANSCAN AS-414 Ultrasonic Flaw Detector (UFD) with integrated analysis software. This device offers high accuracy in evaluating material characteristics and enables correlation of ultrasonic velocity with nodularity in SG iron castings. A 10 mm diameter transducer probe with a frequency of 4 MHz was used to generate and receive ultrasonic waves.

4.1 Principle of Ultrasonic Velocity Measurement

Ultrasonic velocity is determined by the Equation (2), as the ratio of specimen thickness (d) to the time (t) taken for the ultrasonic wave to travel through the material[11]:

$$UV = \frac{d}{y} \tag{2}$$

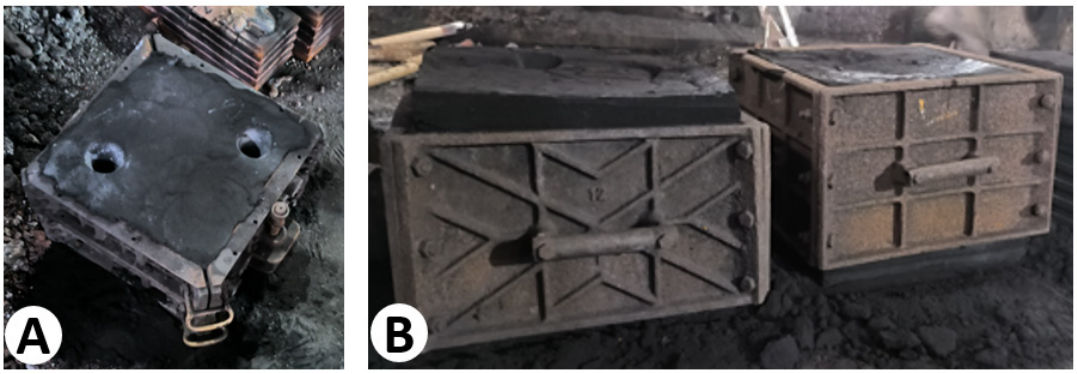


Figure 2. Molding operation **(A)** Preparation of cope **(B)** Addition of mold jacket.

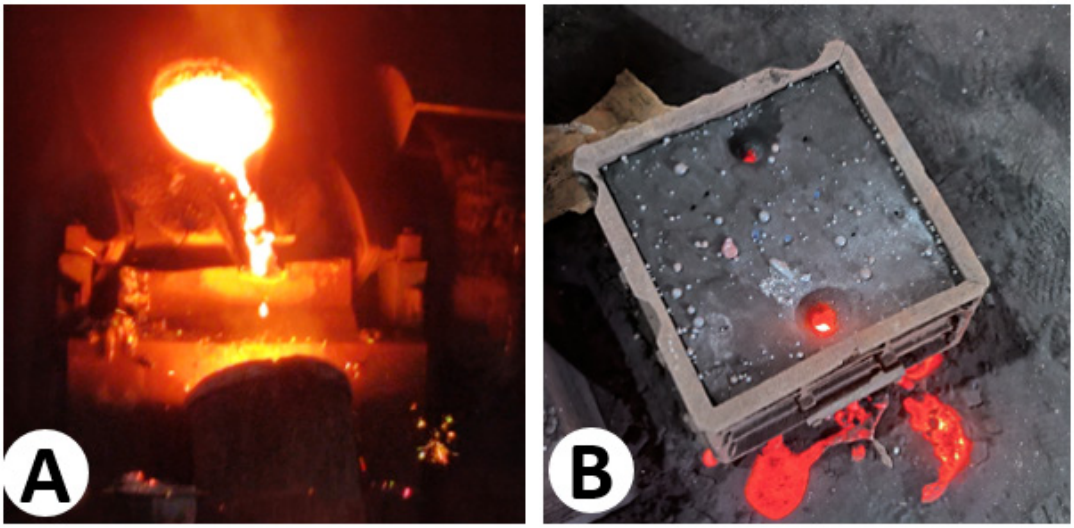


Figure 3. Pouring operation **(A)** Melting **(B)** Mold after pouring.

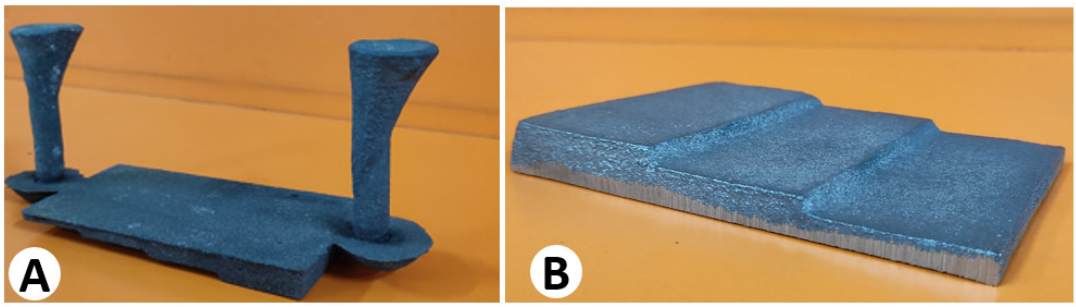


Figure 4. **(A)** Step Casting Bunch **(B)** Step casting after fettling.

The velocity of sound in a material depends on its density, elasticity, and internal microstructural features. In SG iron, ultrasonic velocity is directly affected by the shape and distribution of graphite nodules, making it an effective parameter for nodularity analysis. Ultrasonic testing can be used for different material characterization as shown Table 5[12].

4.1.1 Calibration of ultrasonic equipment

To ensure precise velocity measurements, calibration was performed using a V2 calibration block made of a material with a known sound velocity of 5890 m/s. The following steps describe the calibration process[13].

Table 5. Relationship between ultrasonic parameters and material characteristics

S. No.	Ultrasonic Testing Parameter	Corresponding Output Parameters
1	Velocity	Component thickness, porosity distribution, and pore dimensions.
2	Attenuation	Grain structure, presence of inclusions, porosity, and micro-cracks.
3	Backscatter amplitude	Grain size and presence of micro-cracks.
4	Acoustic	Volumetric or bulk material features.

1. Preparation: Initially 4 MHz probe is attached to the ultrasonic flaw detector. The couplant is then applied between the probe and the V2 block to ensure effective signal transmission.
2. Initial setup: The Gate1 has been set on the back-wall echo of the V2 block. Then the velocity value is adjusted in the system to 5890 m/s, the standard for the V2 block material.
3. Verification: The displayed thickness should read 12.5 mm, matching the actual thickness of the V2 block. If the reading deviates, adjust the probe zero until the thickness displayed matches 12.5 mm.
4. Final confirmation: Once the reading stabilizes at 12.5 mm, calibration is complete.

4.2 Ultrasonic Velocity Measurement Procedure

After calibration, the ultrasonic velocity of SG iron specimens (SGI 400/12, SGI 500/7, and SGI 600/3) was measured. The procedure followed these steps[13].

4.2.1 Sample Preparation

Surface preparation included hand polishing to minimize surface roughness and enhance signal clarity. SG iron samples were prepared to ensure consistent measurements.

4.2.2 Probe Placement

The probe was placed on the sample surface, and an oil as couplant was applied to ensure optimal contact.

4.2.3 Signal Acquisition

Gate 1 was set to the specimen's back-wall echo. The software recorded the ultrasonic velocity. Adjustments for step castings: As the initial thickness reading differed from 5 to 15 mm, the velocity setting was adjusted until the reading displayed as per actual sectional thickness. The adjusted velocity value was noted as the material's ultrasonic velocity[14,15]. For repetition for accuracy, each sample was tested multiple times to ensure consistency in the measurements.

The step-casting samples, with thicknesses of 5 mm, 10 mm, and 15 mm, were tested at 3 pre-determined locations for each thickness to assess ultrasonic velocity and nodularity as shown in Figure 5. A 4 MHz probe was

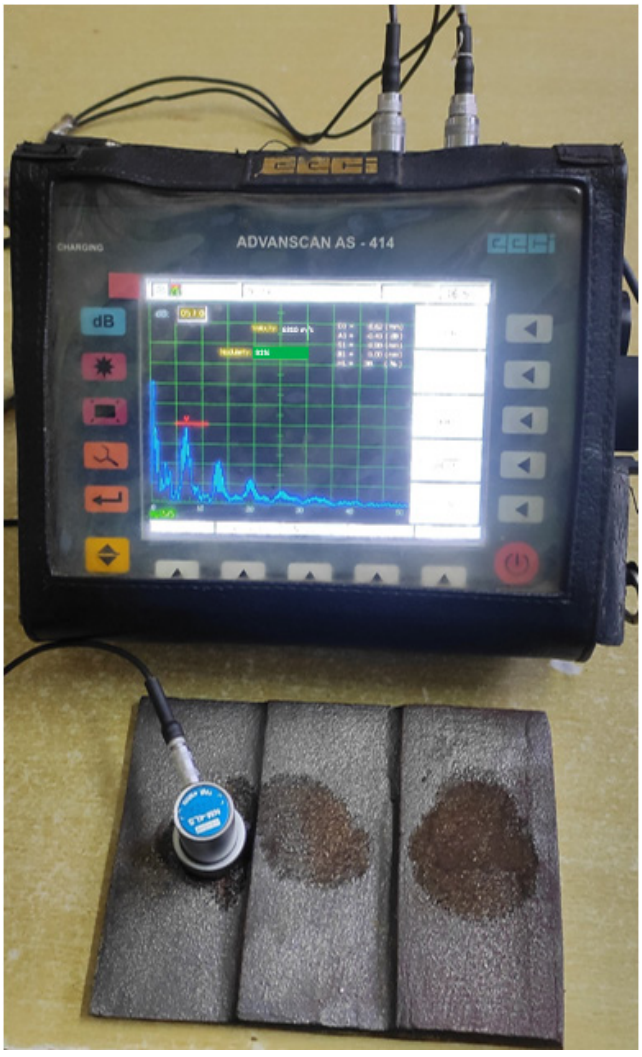


Figure 5. Assessment of ultrasonic velocity and nodularity of the step-casting by flaw detector.

systematically positioned at each location, starting from the thinner 5 mm step and progressing to the thicker 10 mm and 15 mm steps. To ensure effective signal transmission and reduce surface-related errors, oil was applied as a couplant between the probe and the sample surface.

At each location, two critical parameters were recorded: V by UFD, the ultrasonic velocity displayed for the sample by the flaw detector; and % Nodularity, the nodularity percentage calculated and presented by the ultrasonic flaw detector software. For accuracy and consistency, three successive readings were taken for each thickness, as A, B, C. Table 6 represents the velocity and nodularity readings of the step-casting for different CEV of 400/12, 500/7 and 600/3 grades of SGI.

The influence of thickness variations on ultrasonic velocity and nodularity was then analyzed. The recorded data highlighted the variations in ultrasonic velocity and nodularity across the steps, which were systematically tabulated and used for comparative analysis[16].

Table 6. The velocity and nodularity readings of the step-casting

Expt No.	PT (°C)	CEV	T (mm)	% Nodularity				Ultrasonic Velocity (Flaw Detector, m/s)			
				A	B	C	Mean	A	B	C	Mean
1	1380	4.6	5	76	77	75	76	5363	5372	5370	5368.3
2	1380	4.6	10	77	78	76	77	5470	5480	5465	5471.7
3	1380	4.6	15	78	77	76	77	5470	5460	5468	5466
4	1380	4.3	10	87	88	86	87	5645	5650	5642	5645.7
5	1380	4.3	15	88	89	87	88	6018	6025	6015	6019.3
6	1380	4.3	5	90	89	91	90	5645	5650	5642	5645.7
7	1380	4	15	91	90	92	91	6114	6120	6125	6119.7
8	1380	4	5	92	93	91	92	6315	6320	6310	6315
9	1380	4	10	94	93	94	93.7	6114	6120	6118	6117.3
10	1400	4.6	5	75	76	74	75	5363	5370	5365	5366
11	1400	4.6	10	77	78	76	77	5470	5480	5465	5471.7
12	1400	4.6	15	78	77	76	77	5470	5460	5468	5466
13	1400	4.3	10	89	90	88	89	5645	5650	5642	5645.7
14	1400	4.3	15	88	89	87	88	6018	6025	6015	6019.3
15	1400	4.3	5	90	89	91	90	5645	5650	5642	5645.7
16	1400	4	15	92	93	91	92	6114	6120	6125	6119.7
17	1400	4	5	93	92	94	93	6315	6320	6310	6315
18	1400	4	10	94	93	94	93.7	6114	6120	6118	6117.3
19	1420	4.6	5	75	76	74	75	5363	5370	5365	5366
20	1420	4.6	10	77	78	76	77	5470	5480	5465	5471.7
21	1420	4.6	15	78	77	76	77	5470	5460	5468	5466
22	1420	4.3	10	88	89	87	88	6018	6025	6015	6019.3
23	1420	4.3	15	89	90	88	89	6018	6025	6015	6019.3
24	1420	4.3	5	91	90	92	91	5645	5650	5642	5645.7
25	1420	4	15	92	93	91	92	6114	6120	6125	6119.7
26	1420	4	5	93	92	94	93	6315	6320	6310	6315
27	1420	4	10	94	93	94	93.7	6114	6120	6118	6117.3
A, B, C- Three successive readings											

5.0 Regression Analysis

To establish a quantitative relationship between nodularity and ultrasonic velocity, regression analysis was performed using the experimental data[17]. The analysis aimed to develop predictive models correlating the percentage nodularity with ultrasonic velocity values obtained from the flaw detector. A linear regression model was formulated, considering the data (average values) from Table 6 ultrasonic velocity (flaw detector, Vf) as the independent variable and Nodularity (N) as the dependent variable. The resulting equation for the regression model is as follows by Equation (3):

$$\% N = 230.2 + 0.0028\ PT - 30.23\ CEV + 0.029\ T - 0.00316\ V_f \quad (3)$$

With, R-sq 0.8955, R-sq (adj) 0.8765, Where, % N- percentage Nodularity, PT- Pouring Temperature (°C), CEV- Carbon Equivalent Value, T- Section Thickness (mm), V_f- Ultrasonic Velocity given by Flaw Detector (m/s)

6.0 Result and Discussion

The experimental results indicate a clear relationship between nodularity, ultrasonic velocity, and microstructural properties of SG iron samples across varying conditions.

6.1 Effect of Carbon Equivalent Value (CEV)

A higher CEV (4.6) consistently produced lower nodularity (74-78%) across all section thicknesses, as reflected in both ultrasonic velocity measurements (5363-5480 m/s). Conversely, a lower CEV (4.0) achieved superior nodularity (91-94%) and ultrasonic velocities (6114-6320 m/s), the nature of relationships are shown in Figure 6-8, confirming the critical role of carbon content in graphite morphology and mechanical properties.

6.2 Influence of Pouring Temperature and Section Thickness

The pouring temperature significantly impacted the microstructure. At 1380° C, the nodularity and ultrasonic velocity were slightly higher than at 1400° C and 1420° C, suggesting slower cooling rates enhanced graphite sphericity. Section thickness also influenced nodularity, with thinner sections (5 mm) showing higher ultrasonic velocities and nodularity percentages compared to thicker sections (15 mm), likely due to faster cooling and refined graphite structure in thinner regions.

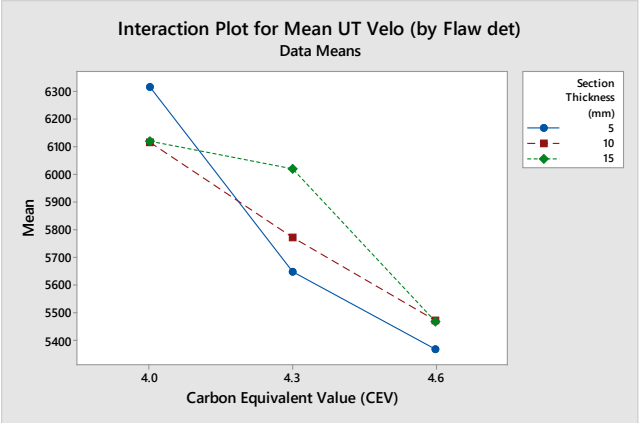


Figure 6. Relation between ultrasonic velocity and CEV.

1. Lower CEV (4.0) is associated with higher ultrasonic velocities (6114-6320 m/s), indicating better material integrity and microstructural refinement.
2. Higher CEV (4.6) results in lower ultrasonic velocities (5363-5480 m/s), reflecting coarser graphite structures and possibly degraded mechanical properties.
3. Thinner sections (5 mm) always have higher velocities, due to faster cooling rates leading to finer microstructure.
4. The interaction suggests that CEV and section thickness jointly influence ultrasonic sound transmission, being closely related to graphite morphology.

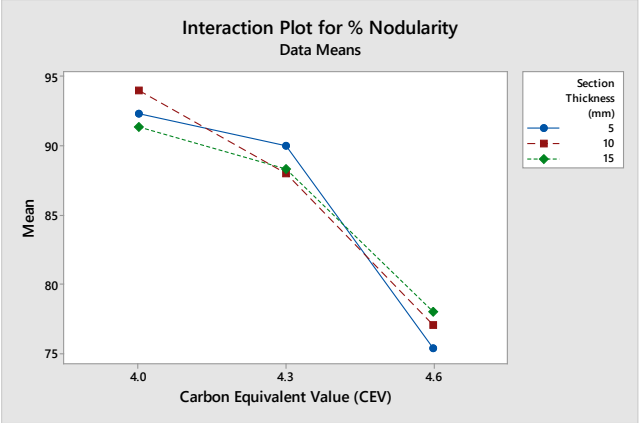


Figure 7. Relation between % nodularity and CEV.

1. Lower CEV (4.0) produces higher nodularity (91-94%) across all section thicknesses, indicating improved graphite spheroidization.
2. Higher CEV (4.6) leads to lower nodularity (74-78%), due to excess carbon promoting flake or irregular graphite.
3. Thin sections (5 mm) demonstrate slightly higher nodularity, indicating improved cooling and nodularity of graphite nodules.
4. The graph points out that both CEV and section thickness has a major influence on the quality of graphite nodules.

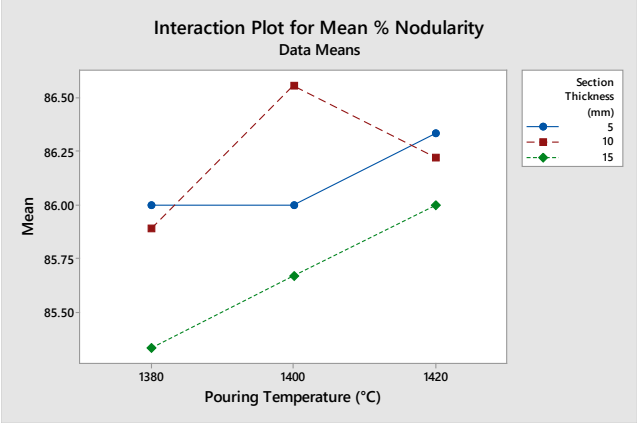


Figure 8. Relation between % nodularity and pouring temperature.

1. As pouring temperature increases, nodularity increases, with increased graphite nodularity at 1420° C.
2. Thinner sections (5 mm) show higher nodularity compared to thicker ones, again due to more rapid cooling.
3. This plot highlights the combined influence of thermal conditions and geometry on final microstructure.

6.3 Validation of Nodularity Measured by Ultrasonic Testing

The microstructures of SG Iron samples of grade 400/12, grade 500/7, and grade 600/3 were examined under an inverted metallurgical microscope. This test was to visually inspect the morphology of the graphite, that is, the nodularity, which is a major factor in the determination of the mechanical properties of spheroidal graphite iron. The samples were observed at 100x magnification to assess the distribution of the graphite nodules within different grades. Out of 27 samples, representative microstructures of SG Iron samples 1 to 9, as presented in Figure 9, were taken with an inverted metallurgical microscope. The images are visual confirmation of graphite morphology and nodularity levels for variable grades and processing conditions.

The strong correlation between nodularity and ultrasonic velocity was validated by both microscopic analysis and flaw detector measurements results as tabulated in Table 7. While minor variations were observed between the 2 methods, the trend remained consistent.

Statistical analysis confirmed a linear relationship between nodularity and ultrasonic velocity, with higher velocities observed in samples with higher nodularity percentages, reinforcing the reliability of ultrasonic testing for non-destructive nodularity assessment.

7.0 Conclusions

This research for SG iron castingsanalysis, confirms a strong positive correlation between nodularity and ultrasonic velocity.

The regression model accommodates high accuracy ($R^2 = 0.8955$) that includes process parameter as pouring temperature, material parameter as carbon equivalent value, anddimensional parameter as section thickness.

It observed that nodularity was greatly improved by lower CEV and higher pouring temperatures, whereas section thickness had only a slight impact.

Further it also confirms the method's dependability by using microscopic observations and ultrasonic test results.

Comprehensively, ultrasonic testing proves to be a rapid, cost-effective, and accurate technique for non-destructive nodularity evaluation in case of S G iron casting. The study recognises that factors such as microstructural heterogeneity, transducer sensitivity, and minor experimental variations may influence predictive accuracy, highlighting the importance of controlled testing conditions and careful parameter selection in subsequent research.

8.0 Acknowledgement

The authors admit that a portion of the approach described is consistent with the procedure revealed in

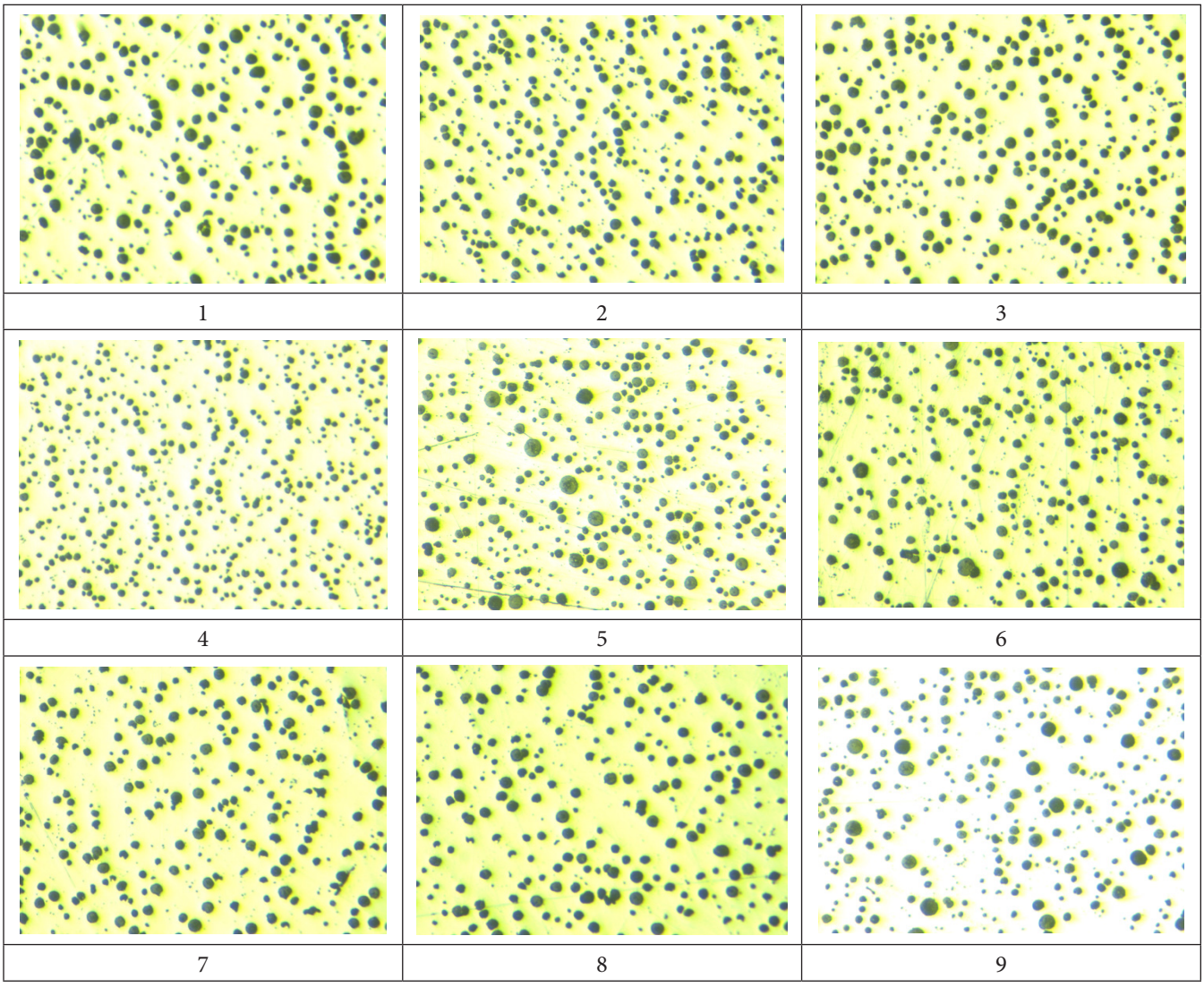


Figure 9. Microstructures of samples 1-9 (captured by inverted microscope at 100x).

Table 7. Validation of nodularity measured by ultrasonic testing

SG Iron Grades	Carbon Equivalent Value (CEV)	Section Thickness (mm)	Ultrasonic Velocity (m/s) by Flaw Detector	% Nodularity (by Flaw Detector)	% Nodularity (by Microstructure Analysis)
400/12	4.6	5	5363	76	75.33
		10	5470	77	77
		15	5470	77	78
500/7	4.3	5	5645	90	87.34
		10	5645	89	88.33
		15	6018	89	89
600/3	4	5	6315	93	91.33
		10	6114	94	92.33
		15	6114	92	94

Patent No. 202521031317, which was published on April 11, 2025 by the authors.

9.0 Author Contributions

Author 1 conducted the experiments, data collection, and drafting the manuscript. Author 2 provided conceptual guidance, supervised the research, and critically reviewed the manuscript. All authors have read and agreed to the published version of the manuscript.

10.0 References

1. Benini L, de Paula PPR, Tavares SSM, *et al*. Evaluation of austempered ductile Iron end milling by magnetic barkhausen noise and x-ray diffraction methods. J Mater Eng Perform. 2025; 34:9026-9036. https://doi.org/10.1007/s11665-025-10794-6
2. Mohan HK, Devaraj S, Swamy KSN, Venkatesh BK. Microstructure and tribological property correlations of die cast and spray formed Al-30 wt.% Si alloy. J Mines Met Fuels. 2023; 70(10A):307-313. https://doi.org/10.18311/jmmf/2022/32772
3. Kadam S, Kabnure B, Mhamane D. Computer-aided simulation of railway insert for defect analysis and yield improvement. J Inst Eng (India) C. 2021; 102:651-656. https://doi.org/10.1007/s40032-021-00680-0
4. Hatate M, Nobuki T, Komatsu S. Accuracy improving methods in estimation of graphite nodularity of ductile cast iron by measurement of ultrasonic velocity. STCP. InTech. 2012. https://doi.org/10.5772/50596
5. Kabnure BB, Shinde VD, Kolhapure RR. Optimization to develop multiple response microstructure and hardness of ductile iron casting by using GRA. J Inst Eng India Ser D. 2018; 99:235-243. https://doi.org/10.1007/s40033-018-0161-8
6. Fikrat Y. Wear studies on phenolic brake-pads using Taguchi technique. Tribol Ind. 2021; 43(3):489-499. https://doi.org/10.24874/ti.1024.12.20.03
7. Nanekar P, Shah BK. Characterization of material properties by ultrasonic. BARC Newsletter. 2003; 249:25-38.
8. Mhamane D, Bewoor A. Ultrasonic testing: Comprehensive approach to forecast mechanical properties of castings. High-performance Sustainable Materials and Structures. SUCI. Springer; 2024. p. 201-211. https://doi.org/10.1007/978-3-031-72527-2_17
9. Regordosa AR, Isern NL, Sertucha J, Lacaze J. Evolution of shrinkage with carbon equivalent and inoculation in ductile cast irons. Mater Sci Forum. 2018; 925: 28-35. https://doi.org/10.4028/www.scientific.net/MSF.925.28
10. Brown JR. Foseco ferrous Foundryman's handbook. 10th ed. Butterworth-Heinemann. 2000.
11. McDonald MR, Gaines SN, Diederichs MS. Interpreting ultrasonic pulse velocities and elastic properties of lac du bonnet granite under compression. IOP Conf Ser Earth Environ Sci. 2023; 1124:012035. https://doi.org/10.1088/1755-1315/1124/1/012035
12. Muthmari S, Singh A. Review of various ultrasonic techniques employed in modern industries. Int J Eng Sci Tech 2011; 3(4):3078-3085
13. Maggi LE, Silva CER, Alvarenga AV, Felix RPBC. Ultrasonic calibration and certification of V1 and V2 type reference standard blocks for use in non-destructive Testing. J Phys Conf Ser. 2011; 279:012029. https://doi.org/10.1088/1742-6596/279/1/012029
14. Agnoletto D, Lemos GVB, Beskow AB, Lessa CRL, Reguly A. Methodology for determination of degree of nodularity in a ductile cast iron GGG 40 by ultrasonic velocity test. South Braz J Chem. 2018; 26(26):10-16. https://doi.org/10.37633/sbjc.26(26)2018.10-16
15. Castellano A, Mazzarisi M, Campanelli SL, Angelastro A, Fraddosio A, Piccioni MD. Ultrasonic characterization of components manufactured by direct laser metal deposition. Materials. 2020; 13(11):2658. https://doi.org/10.3390/ma13112658
16. Mhamane DA, Bewoor AK, Mhamane RD, Bewoor LA. Process for predicting nodularity, material properties in SG iron castings using simulation and ultrasonic testing. 2025.
17. Charoenvilaisiri S, Stefanescu DM, Ruxanda R, Piwonka TS. Thin wall compacted graphite iron castings. Trans Am Foundry Soc. 2002; 110:1113-1130.